Contents lists available at Science-Gate

International Journal of Advanced and Applied Sciences

Journal homepage: http://www.science-gate.com/IJAAS.html

Solidity investigation of microgrid in islanding operation

T. Yuvaraja [1,*], G. Sundar [2], S. Arumugam [3]

[1]Department of EEE, Meenakshi Academy of Higher Education and Research, (MAHER University), Chennai City, India
[2]Department of EEE, Arulmigu Meenakshi Amman College of Engineering, Vadamavandal, Kanchipuram, Tamil Nadu State, India
[3]GRT Institute of Engineering and Technology, Tirupathi Highway, Mahalakshmi Nagar, Puzhal, Chennai City, Tamil Nadu State, India

ARTICLE INFO

Article history:
Received 26 April 2016
Received in revised form
16 June 2016
Accepted 17 June 2016

Keywords:
Fuzzy control
Static VAR compensator
Inverter
FMRLC
Voltage source converter

ABSTRACT

Several pioneering organize techniques has been incorporated for attractive the steadiness of Microgrid as meant for proper load allowance. The hefty amount all-purpose method is to apply of droop distinctiveness for decentralized load sharing. Analogous converter has been proscribed to dispense much loved real power and reactive power en route for the design. Narrow singles are worn as reaction to control converters, in view of the fact that in a real system, the detachment between the converters could build the inter-communication impracticable. The real and reactive power sharing container is achieved by calculating two independent quantities frequency furthermore voltage extent. The plan of this development is to develop a dynamic reproduction of a converter fed Microgrid and intend a control scheme to legalize its voltage and frequency in the islanded mode of operation. A controller reminiscent of PI, FUZZY, FUZZY-PI, FMRLC-Algorithm to be implemented to excellent which is best controller for the developed operation control network. Voltage source converter (VSC) is of the essence for controlling the Microgrid so a single phase inverter is residential in hardware.

1. Introduction

Disseminated generation positioned in close proximity to to demand distributes electricity with trifling losses. This power may consequently have a higher value than power imminent from large, central conventional generators through the outmoded utility transmission and distribution infrastructure. With the usage of renewable disseminated generation, the enslavement on fossil fuels and other conventional sources and their price can be a bridged (Yuvaraja and Gopinath, 2015a). This step will furthermore go ahead to a vital diminish of carbon dioxide emanations, which is indispensable in plentiful statute programs.

However, beneath today's griding codes, all thin production, whether non conventional otherwise fossil-fueled, necessitate shut downstairs premeditated for the period of efficacy grid power outages (Yuvaraja and Gopinath, 2015a).This is exactly when these on-site sources may perhaps the greatest value to both generation proprietors and civilization (Yuvaraja and Gopinath, 2015b).

A microgrid is a provincially limited energy system of distributed energy resources, customers and optionally storage. It augments one or many of the following: Power quality and steadiness, sustainability and fiscal welfares and it may continuously lope in off-grid- before on-grid mode, as well as in Siamese twin mode by shifting the grid connection position (Lasseter and Paigi, 2004). According to this categorization, a microgrid exploits the welfares of distributed generators and deciphers the above cited drawback, also utilizing distributed generation during utility power system outages.In grid-connected mode, the microgrid machinist can take pecuniary conclusions – such as to vend or procure energy contingent on on-site generation proficiency, its cost, and the presented prices on the vigor advertise (Martin et al., 1995). In incident of a helpfulness power system outage, the point-of-common- coupling tidal wave motivation robotically open, and creature generators will prolong to supply power to masses contained by the microgrid.The acquaintance on microgrids is not original. In the underpinning of idyllic electrification, abundant microgrid edifices have be installed. Later, the economic aids of an organized utility grid with large power plants led to today's power scheme structures (Oshima et al., 1991).

2. System structure and converter model

* Corresponding Author.
Email Address: yuvarajastr@gmail.com (T. Yuvaraja)

The designed sector designates the arrangement of a simple microgrid, shown in Fig. 1. It entails a collector bus, a voltage source converter, a bus capacitor, C_B, along with the load (Woyte et al., 2003). The capacitor Connected along with the load ensures that the voltage pulsations at the terminuses of the voltage source converter do not seem across the load (Ropp et al., 1999). For minimalism, the load is estimated to be unprejudiced, and it is characterize as a parallel amalgamation of resistance R and inductance L, as is the standard in islanding detection narrative (Kotsopoulos et al., 2002). The line impedance sandwiched between the collector bus and the load is less significant than the load impedance and is abandoned. The converter is associated with the collector bus through an interface inductor, which is not revealed here (Smith et al., 2000).

It is assumed in this paper that:

1. The converter output parameters are controlled by controlling the pulse given to the gate terminal and Switching is done through pulse width intonation.
2. The operating frequencies of the voltage source converter switches are able-bodied above the fundamental frequency of the ac supply and the resonant frequency of the microgrid.
3. The dc state of the converter is allied to a strong dc bus with amply towering voltage.
4. The converter is regulated by a sky-scraping bandwidth current controller.
5. The complete system is considered to be in balanced condition.

By assuming these conventions, the fundamental frequency of the Voltage Source converter model is justified; and somewhere the converter exhibits as a middling current resource. Note that the high frequency converter current dynamics have been snubbed in order to focus solely on the dynamics and control of the islanded microgrid.

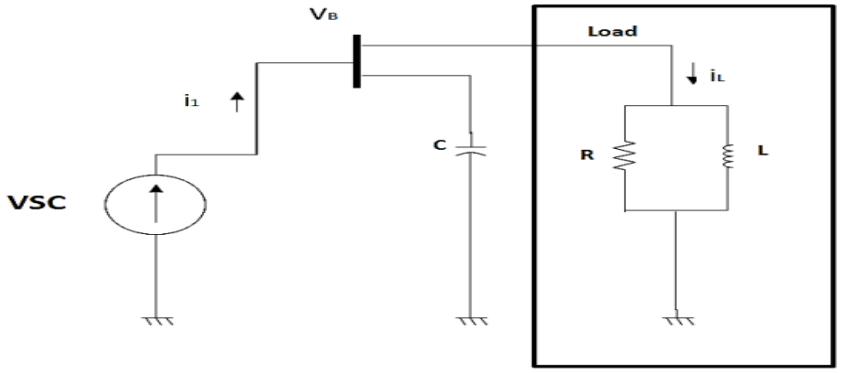

Fig. 1: A converter fed power network in islanded mode

2.1 PI Controller

It is quantified in that the rotating reference frame system voltage is swayed into stationary reference frame by the active current i_{1d} whereas the reactive current i_{1q} impetuses the frequency. This fragment endorses a control structure that hires i_{1d} and i_{1q} as control input to legalize the V_{Bd} and ω_B correspondingly. Subsequently the dynamics of the coordination voltage and frequency are coupled. Thus, the subsequent methodical tactic is used in evolving the control scheme to guarantee closed loop stability in the manifestation of both voltage and frequency control loop compensators: Originate the transfer function approach that relates i_{1d} to V_{Bd}. Decide on the parameters of first PI compensator for the Voltage control loop. Augment the system exemplary with the compensator equation. Use the improved system exemplary to start off the transfer function that relates i_{1q} to ω_B. Decide on the parameter of a second PI compensator for the frequencies have power over loop, by the side of with a virtual damping resister Rv.

2.2 Voltage Control

The linearized system exemplary of may be castoff as the introductory fact for the derivation of the plant transfer function relating i_{1d} to V_{Bd}. Setting i_{1q} = 0 and reordering the blocks fallouts in the plant model which may be rationalized to originate the succeeding transfer function (Eq. 1):

$$\frac{V_{Bd}(s)}{i_{1d}(s)} = \frac{s^2/C_B - K_P K_I/C_B}{s^3 + s^2/RC_B + \left(2/LC_B - K_P K_I\right)s - K_P K_I/C_B} \quad (1)$$

It can be shown by means of Routh-Hurwitz criterion that the open loop transfer function would be unhinged if the coefficient factor KPKI were positive. While KPKI may be confirmed to be negative irrespective of the value of i1q and i1d, the damping of the open loop scheme is contingent upon the load. As the load diminutions, coefficient 1/RCB and KPKI /RCB approaches zilch, moving the system poles towards the imaginary axis. To keep the open loop system adequately damped irrespective of load resistance, a virtual resistance Rv is added in parallel with CB. This is comprehended by creating i1d a function of VBd as well as the compensator output uv. The reformed transfer function as seen by the compensator is (Eq. 2):

$$\frac{V_{Bd}(s)}{U_V(s)} = \frac{s^2/C_B - K_P K_I/C_B}{s^3 + s^2/RC_B + \left(2/LC_B - K_P K_I\right)s - K_P K_I/C_B} \quad (2)$$

In view of the fact that constants 1/ReCB and during the transfer function of (2) is always greater

than 1/RvCB and, KPK_I/ReCB the scheme is well damped nevertheless of the load resistance. Devising confirmed that the plant is well damped, a PI compensator may be castoff to outcome the system voltage to track the voltage allusion V*Bd. The direct input is (Eq. 3):

$$u_v(s) = \left(K_{Pv} + \frac{K_{iv}}{s}\right)\left(v_{Bd}{}^*(s) - v_{Bd}(s)\right) \quad (3)$$

Where K_{pv} and K_{iv} are proportional and fundamental gains equally. The blocked loop transfer function of the voltage control loop is (Eq. 4 and 5):

$$\frac{v_{Bd}(s)}{v_{Bd}{}^*(s)} = \frac{(K_{pv}s+K_{iv})\left(\frac{s^2}{C_B}-\frac{K_PK_I}{C_B}\right)}{D(S)} \quad (4)$$

Where

$$D(S) = S^4 + \left(\frac{1}{R_eC_B} + \frac{K_{pv}}{C_B}\right)S^3 + \left(\frac{2}{LC_B} - K_PK_I + \frac{K_{iv}}{C_B}\right)S^2 - \left(\frac{K_PK_I}{R_eC_B} + \frac{K_PK_IK_{pv}}{C_B}\right)S - \frac{K_PK_IK_{pv}}{C_B} \quad (5)$$

The proportional and integral gains of compensator are preferred as 0.078 and 95 correspondingly plus the step response of the voltage control loop for two load configuration as generated by MATLAB/Simulink is shown below.

2.3 Frequency Control Scheme

As both the voltage and frequency of the microgrid are controlled, the system consummate of Fig. 2, which includes the voltage controller, is hand-me-down for the derivation of $\omega_B(s)/i_{1q}(s)$. Fig. 2 shows that transfer function $\omega_B(s)/i_{1q}(s)$ is given by (Eq. 6 and 7):

$$\frac{\omega_B(s)}{i_{1q}(s)} = -K_b\frac{v_{Bd}(s)}{i_{1q}(s)} + \frac{1}{C_Bv_{Bd0}}\left(\frac{i_{Lq}(s)}{i_{1q}(s)}\right) \quad (6)$$

Deriving transfer function and substituting them in (5) results in:

$$\frac{\omega_B(s)}{i_{1q}(s)} = -\frac{\frac{k_bK_as^2}{C_B}}{D(s)} + \frac{D(s)-k_IK_as^2+\left(\frac{k_IK_a}{RC_B}+\frac{k_IK_aK_{pv}}{C_B}\right)s-\frac{k_IK_aK_{iv}}{C_B}}{C_Bv_{Bd0}D(s)} \quad (7)$$

The denomination of $\omega_B(s)/i_{1q}(s)$ is one and the same to that of the closed loop transfer function of the (4), which is balanced and glowing damped. This entails in the isolation of the purpose of the frequency control loop has a stable plant and a PI compensator may be castoff to normalize the system frequency to track ω_B*.

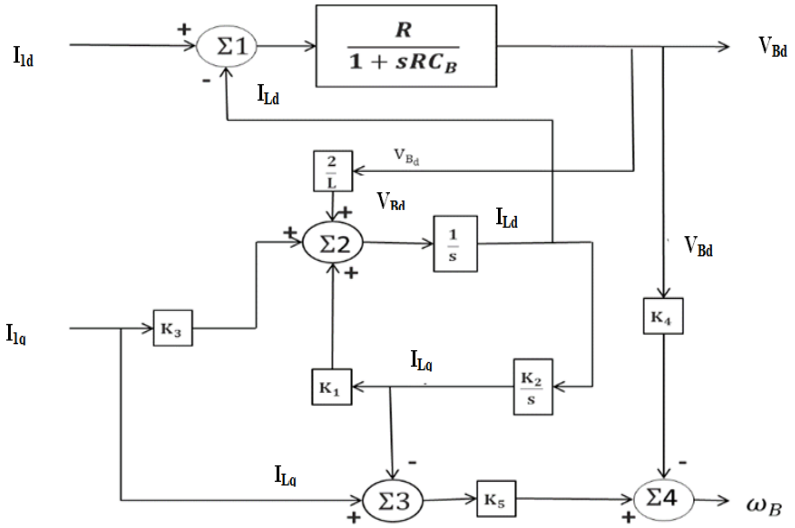

Fig. 2: Linearized system model with the voltage control loop added

A frequency control loop is anticipated for the power system. The stand constraints and the linearization position are manipulated. The comparative and fundamental gain of the reparation is chosen as 0.014 and 17 respectively and the step responses of frequency control loop for two load configuration.

2.4 Fuzzy Controller

Fuzzy systems are widely used in today engineering (Saber et al., 2014; Kadir, 2014; Anderson 2015; Sangsefidi et al., 2015; Hofford 2015; Markez and Pique, 2015). In control, based on conventional PI control method, the modernized fuzzy control algorithm is cast-off to assess the fuzzification and defuzzification progression in MATLAB/Fuzzy toolbox. The variables and its associate membership function of fuzzy toolbox is created. By instigating the fuzzy technology the voltage and frequency can be controlled in a single controller, the inaccuracy from voltage and frequency is given to the fuzzy controller and the output gain is given to the plant from the controller. Inputs to the fuzzy controller are voltage error and frequency error. And the outputs from the fuzzy controller are I1d and I1q which are the real and reactive power respectively in Fig 3 and 4.

3. PI controller and FMRLC algorithm

A MG in islanded mode is used to verify the performance of proposed FMRLC algorithm. The structure of MG power system used for the simulation is shown in Fig. 5.

Fig. 5 system is composed of PV bus supplied by two sources, wind turbine and asynchronous generator and PQ bus with two loads, linear load and

induction motor. The PV and PQ buses are connected via 100 m distribution line. The wind turbine represents a renewable source.

The asynchronous generator is used as a synchronous condenser that controls the grid voltage by its excitation system during load or/and wind variation.

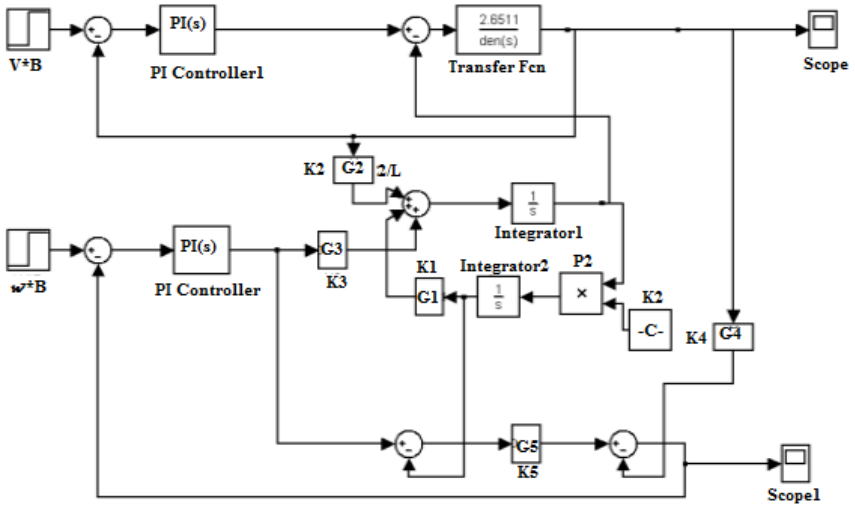

Fig. 3: Shows the MATlab/Simulink diagram of PI Controller Linearized system model

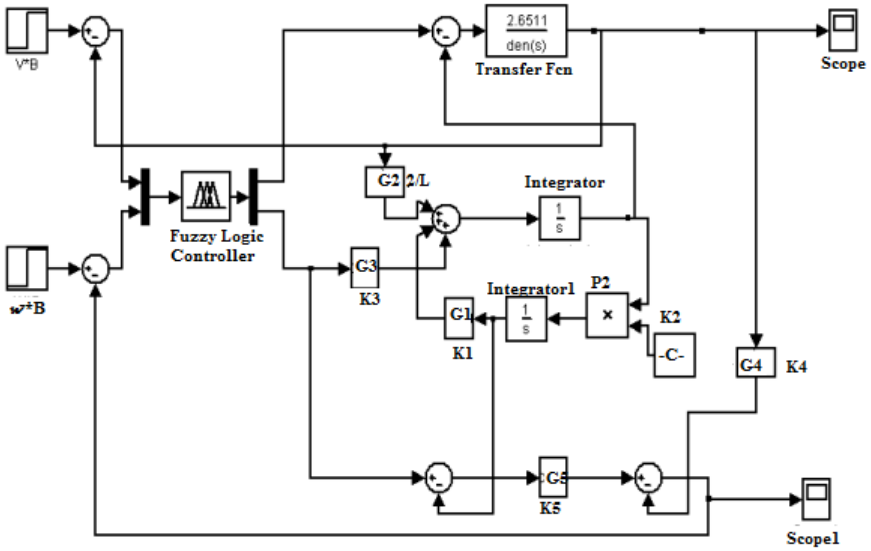

Fig. 4: MATlab/Simulink block diagram for FUZZY Controller

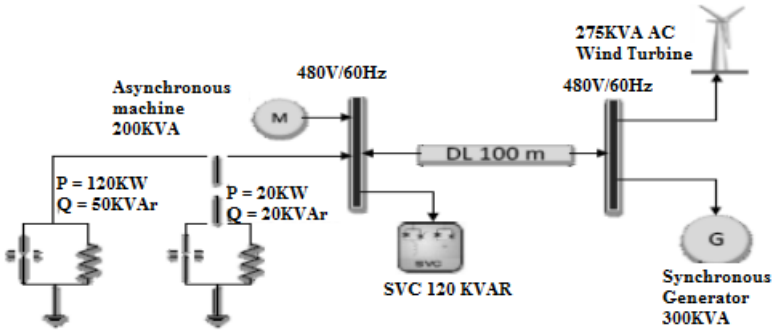

Fig. 5: Single line diagram of the power system used in the simulations

The induction motor is 200kW while the linear load consists of 120 kW active loads and 50 kVAR capacitive loads connected continuously to the bus and 20 kW active loads and 20 kVAR capacitive loads connected after 2.5 seconds of the simulation. A 120 kVAR Static VAR Compensator (SVC) is connected at load side. The mathematical model of the SVC is presented. The simplified SVC phasor model block of the FACTS library of MATLAB/SIMULINK is used for the simulation. The original model of SVC applies PI controller. The controller was modified to switch

between PID conventional control algorithm and FMRLC algorithm.

4. Comparison of simulation results

Comparing Fuzzy and PI controller Output for Voltage Control shown in Fig. 6-Fig. 8. For 'R' load and 'RL' Load.

Comparing Fuzzy and PI controller Output for Frequency Control shown in Fig. 8 for 'RL' load and 'R' Load.

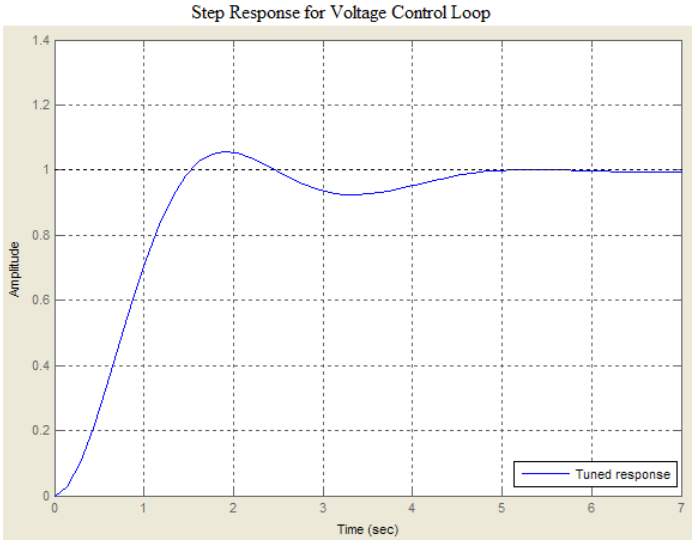

Fig. 6: Fuzzy PI controller output response for voltage control 'R' Load

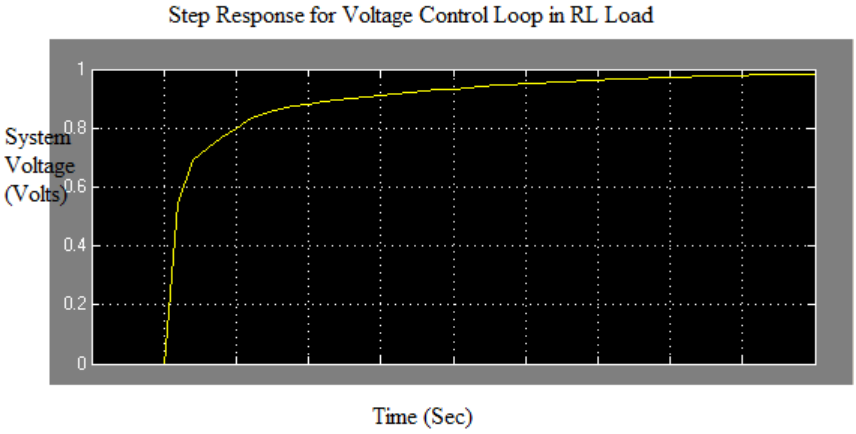

Fig. 7: Fuzzy PI controller output response for voltage control 'RL' Load

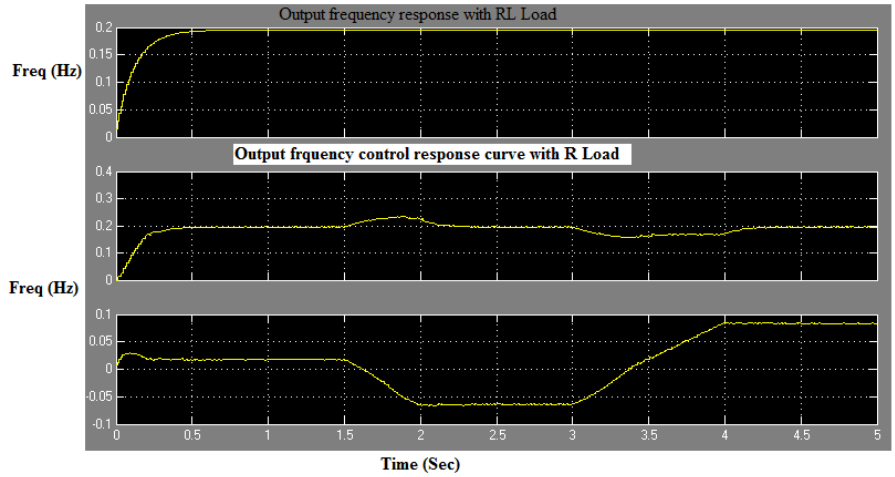

Fig. 8: Fuzzy PI Controller output response for frequency control for 'RL' Load and 'R' Load

The objective of simulations is to verify the enhancement of MG performance in islanded mode using proposed FMRLC against performance of applying a well-known PID controller that is used as a benchmark for comparing different control algorithms. Moreover, to show effectiveness of SVC,

performance of the two control algorithms were compared with MG performance without SVC. In this case, asynchronous generator is used as a synchronous condenser and its excitation system controls the grid voltage at its nominal value. The simulation is conducted using the system described in section 3 for 15 sec. A load change is applied to the induction motor by a repeating pattern as shown in Fig. 9. The objective of the repeating pattern of load change is to expose learning algorithm repeatedly to possible variations that could take place within the power system. Hence, the system would form and memorize proper control surface for different operating points. In addition, a linear load has been connected to MG after 2.5 sec to allow MG to operate on its edge of power follow (the load was not connected at start of simulation to avoid MG instability during its transient). The reference model parameters were calculated from equation (1) and (3). The time constant however, as stated in section 2, a larger time constant of 0.04 sec (about 7 times the calculated one) is used to allow more achievable performance. The selection is confirmed with the results shown in Fig. 10 where the average absolute reactive power from the SVC was 40 kVAR. The required OS% is set to 1%, hence, $\omega_{n=\ 30sec}$. A PID FMRLC was used in control loop of SVC. It was found that PI or PD FMRLC wouldn't perform adequately as it will be shown in results discussion. Eleven membership functions are used for fuzzy controller and five for inverse model. A PID

FMRLC was used in control loop of SVC. It was found that PI or PD FMRLC wouldn't perform adequately as it will be shown in results discussion. Eleven membership functions are used for fuzzy controller and five for inverse model. The simulation result for the first 10 seconds for the proposed PID-FMRLC. Fig. 10 shows the same simulation using PID SVC and without SVC. The scales in Fig. 9 and Fig. 10 are the same for convenience. Top curves, in Fig. 9, show bus voltage (pu) for FMRLC (in solid black line) and reference model in (in dashed blue line) and, for PID controller (in solid black line) and without SVC (in dashed blue line). It can be noted that FMRLC algorithm was able to maintain line voltage to the required level with minimal disturbance compared to both conventional PID controller and simulation without SVC. The transient behaviors of the system follow closely the reference model transient. The second curve in Fig. 9 shows the error between reference model output and measured bus voltage for FMRLC algorithm. The learning algorithm was able to store information about proper control action during grid transient and recall it to minimize error during the full simulation run. On the other hand, PID controller shows steady performance that does not improve with time as expected as shown in second curve in Fig. 10. The grid without SVC has degraded performance.

The bottom curves, in both Fig. 9 and 10, show the measured susceptance of the SVC voltage regulator for both FMRLC and PID controller respectively. In addition the load variation of the induction motor is presented. The proposed PID-FMRLC algorithm was able to generate strong control action and deploy the full capacity of SVC to compensate for load disturbance. The PI controller was not able to generate strong control action despite of it operation close to the critical stability region. The bus voltage and the voltage error in the period from 4.1 sec to 4.6 sec; at time 4 sec, the machine load increased form 0.1 pu to 0.9 pu. The measured overshoot was 0.9% for the FMRLC algorithm while it was 1.2% using the PID controller. Without SVC, the overshoot was 1.8%. The voltage settle within 6% of its maximum deviation from desired bus level after 0.35 sec (four to five times the time constant) for the FMRLC while it takes 2.9 sec with the PID controller.

Integral-of-Time Multiplied Absolute Error (ITMAE) and integral square error (ISE) for the three cases for 16 sec simulation. The measurement of both error parameters (ITMAE and ISE) was performed after the 1st 1.3 sec of simulation to avoid building high values during MG transient operation that would hide the details of system performance during the rest of simulation period.

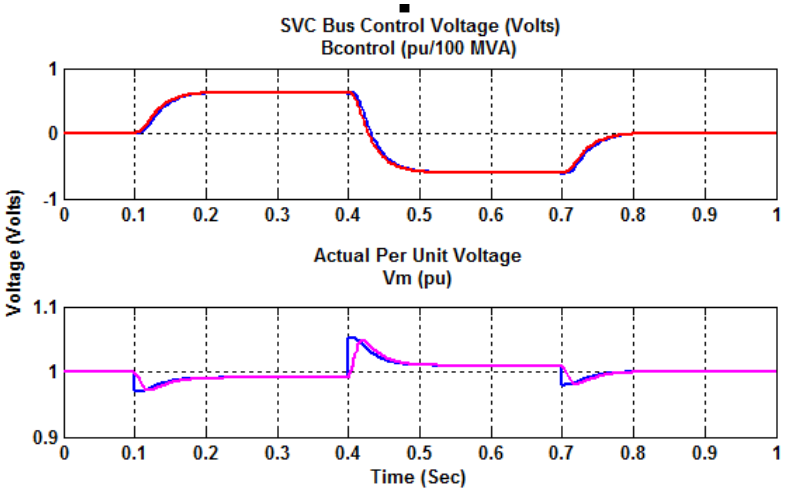

Fig. 9: Measured performance of MG using FMRLC SVC. From top to bottom 2- the bus voltage/reference model output, voltage error between bus voltages and reference model, and 1- the SVC susceptance/Load.

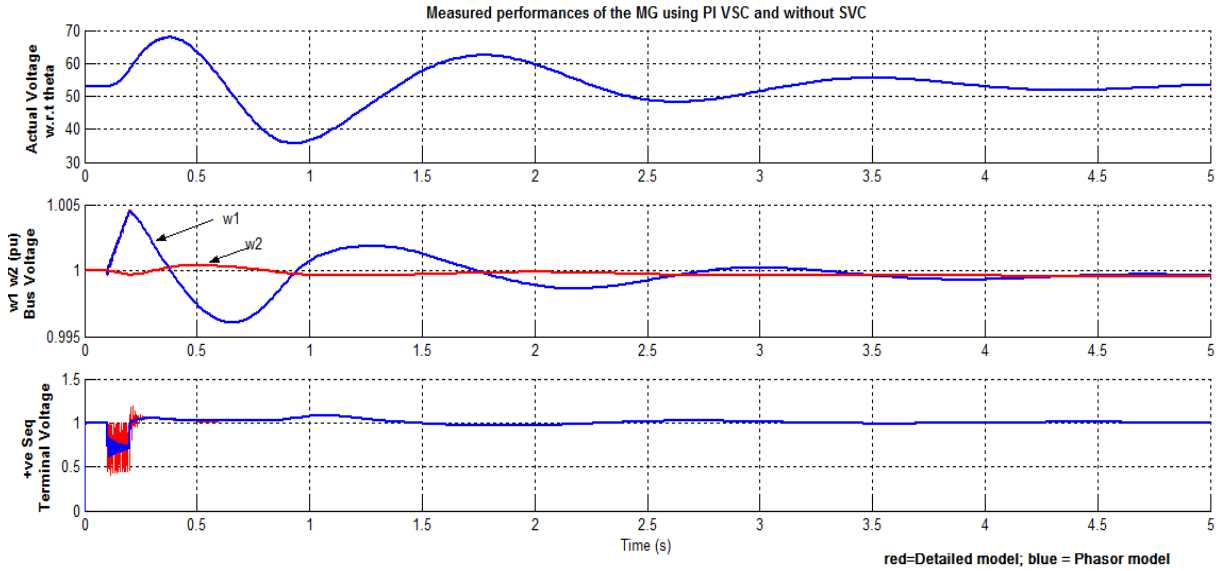

Fig. 10: Measured performances of the MG using PI VSC and without SVC. From top to bottom 1- the bus voltage, 2- voltage error between bus voltages and reference model and 3- the SVC susceptance/Load

5. Conclusion

The relative work and outcomes presented in this plan demonstrates the dynamic model of an islanded microgrid and is formulated in a stationary reference frame that is instantaneously synchronized to the collector bus voltage. The examined model recognizes that the real power balance between the converter and the load determines the microgrid voltage while the frequency depends on the reactive power balance. Based on the urbanized model, a regulatory control structure is amalgamated for a converter with conventional dq frame for the current control. A Fuzzy based controller manipulates the sets of the d-axis current reference to regulate the bus voltage magnitude and the same regulator sets the q-axis current reference to regulate the system bus frequency. Frequency of the point of common coupling voltage is therefore a regulated output of the system. The results comprehended the legitimacy of the model and robustness of the proposed control scheme to changes in system loading and power factor.

References

Christopher Anderson (2015). Learning Algorithm to promote future specialist. International journal of Advanced and Applied Sciences, 2(4):8-13.

Hofford S (2015). Survey of fatigue resistance quantification of asphalt mixture. International journal of Advanced and Applied Sciences, 2(1):42-49.

Kadir T (2014). In discrepancy between the traditional Fuzzy logic and inductive. International journal of Advanced and Applied Sciences, 1(7):36-43.

Kotsopoulos A, Duarte J, Hendrix MAM and Heskes PJM (2002). Islanding behaviour of grid-connected PV inverters operating under different control schemes. In Power Electronics Specialists Conference, 2002. pesc 02. 2002 IEEE 33rd Annual. IEEE. 3: 1506-1511

Lasseter RH and Paigi P (2004). Microgrid: a conceptual solution. In Power Electronics Specialists Conference, 2004. PESC 04. 2004 IEEE 35th Annual. IEEE. 6: 4285-4290.

Markez J and Pique E (2015). Particle swarm optimization in the coefficients a, b of Forchheimer equation. International journal of Advanced and Applied Sciences, 2(3):15-23.

Martins AP, Carvalho AS and Araujo AS (1995). Design and implementation of a current controller for the parallel operation of standard UPSs. In Industrial Electronics, Control, and Instrumentation, 1995., Proceedings of the 1995 IEEE IECON 21st International Conference on. IEEE. 1: 584-589.

Oshima H, Miyazaya Y and Hirata A (1991). Parallel redundant UPS with instantaneous PWM control. In Telecommunications Energy Conference, 1991. INTELEC'91., 13th International. IEEE: 436-442

Ropp ME, Begovic M and Rohatgi A (1999). Analysis and performance assessment of the active frequency drift method of islanding prevention. Energy Conversion, IEEE Transactions on, 14(3): 810-816.

Saber S, Lweis F, Ahmad FAH, Romol NA, Abdul Tawan H, Monir A and Umran M (2014). On the comparison of traffic noise in different countries. International journal of Advanced and Applied Sciences, 1(3):1-10.

Sangsefidi SJ, Moghadasi R, Yazdani S and Mohamadi Nejad A (2015). Forecasting the prices of agricultural products in Iran with ARIMA and ARCH models. International journal of Advanced and Applied Sciences, 2(11):54-57.

Smith GA, Onions PA and Infield DG (2000). Predicting islanding operation of grid connected PV inverters. In Electric Power Applications, IEE Proceedings. IET. 147(1): 1-6

Woyte A, Belmans R and Nijs J (2003). Testing the islanding protection function of photovoltaic inverters. Energy Conversion, IEEE Transactions on, 18(1): 157-162.

Yuvaraja T and Gopinath M (2015). Fuzzy Based Analysis of Inverter Fed Micro Grid in Islanding Operation. International Journal of Power Electronics and Drive Systems, 5(4): 464-469.

Yuvaraja T and Gopinath M (2015). Multiple current control strategies for an optional operation of VSC linked to an ineffectual point in the power system beneath diversified grid conditions. International Journal of Soft Computing. 10(2): 118-126.